sciendo

*Polish Cartographical Review*
*Vol. 54, 2022, pp. 35–53*
DOI: 10.2478/pcr-2022-0004
Received: 25.05.2022
Accepted: 21.07.2022

PAWEŁ PĘDZICH
Warsaw University of Technology
Faculty of Geodesy and Cartography
Department of Cartography
Warsaw, Poland
orcid.org/0000-0001-5292-4887; pawel.pedzich@pw.edu.pl

# Conformal projections of a tri-axial ellipsoid based on isometric coordinates: history, methodology, and examples

**Abstract.** The paper presents a review of the conformal projections of a tri-axial ellipsoid and the methodology of creating these projections with the use of isometric coordinates. The concept is very simple and has been known for a long time; if isometric coordinates are introduced on the surface of the original and on the plane of the image, then any analytical function of the complex variable, i.e. a function that has a continuous derivative, creates a conformal projection. The introduction presents the history of conformal projections. Then, existing projections are presented, including the Bugayevskiy projection and several projections developed by the author that apply selected functions of the complex variable. Scripts were prepared in the Octave software with the use of the presented methodology. Programming in Octave offers a possibility of a simple implementation of complex variable functions, which is also briefly discussed in the paper. The developed scripts were then used to perform calculations and to draw cartographic grids and distortion isolines in the selected conformal projections. The test object was the tri-axial ellipsoid that represents Phobos.

**Keywords:** cartographic projections, conformal projections, conformal coordinates, tri-axial ellipsoid

## 1. Introduction

Conformal projections have been used since the Ancient era and are still used nowadays. They have a wide range of applications, including in creating topographic maps and for numerous other purposes. These projections also play a major role in planetary cartography, which is one of the most interesting and dynamically developing fields of cartography due to the growing interest in the exploration of space and the large amount of data about celestial bodies that are obtained from various space missions. The reference surfaces applied in the projections that are used to map the surface of the Earth or of other large planets are usually an oblate ellipsoid or a sphere. However, a tri-axial ellipsoid seems to be more suitable for preparing maps of such irregular objects as asteroids or small celestial bodies. Currently, an increasing number of publications on this subject appear, including the works of the Russian cartographer Nyrtsov. His research was probably inspired by the works of another Russian cartographer, Lev Moseevich Bugayevskiy, whose studies on the projections of a tri-axial ellipsoid published in the 1980s should be considered as breakthrough works. Bugayevskiy was the author of the method of determining isometric coordinates on a tri-axial ellipsoid and of the cylindrical conformal projections, as well as of numerous other projections (Bugayevskiy, 1987, 1991). The problem of conformal projections of a tri-axial ellipsoid were also analysed by the American scientist John Parr Snyder, who developed a method for calculating so-called conformal coordinates and their application to create this type of projections (Snyder, 1995).

The aim of this paper is to present to the readers the methodology of creating conformal projections of a tri-axial ellipsoid with the use of isometric coordinates. The isometric coordinates were calculated with the use of the formulas developed by Bugayevskiy, which have the form of functions of planetographic coordinates. As the data for multiple extra-terrestrial bodies are often expressed in form of planetocentric coordinates, the knowledge of the methods for converting the coordinates between different systems might be useful. These methods were described, among others, in the works Bugayevskiy (1998) and Pędzich (2017), and the main definitions were also presented in the study by Pędzich and Latuszek (2014). Here, it is worth noting that the planetocentric latitude is the angle between the plane of the equator and the straight line passing through the centre of the ellipsoid and the given point, while the planetographic latitude is the angle between the plane of the equator and the normal to the ellipsoid at a given point.

Apart from the method of calculating the isometric coordinates, the paper also presents sample projections along with an analysis of their properties.

## 2. An outline of the history of conformal projections

### 2.1. Beginnings and the main studies on conformal projections

The oldest known conformal projection is the stereographic projection of a sphere on a plane, which is attributed to Hipparchus and was created about 130 BC. This projection was used by Ptolemy to create a map of the sky in mid-2$^{nd}$ century. Ptolemy also noted an interesting property of this projection, namely that all circles of the sphere are projected to circles on a plane (Biernacki, 1949).

The well-known Mercator's projection was first used in 1569, on his map of the world that consisted of 18 charts joined to create one whole map of the dimensions of 1.3 m by 2 m. Mercator entitled his map *Nova et aucta orbis terrae desciptio ad usum navigantinum emendate accomodata*. It was the first known cylindrical equiangular projection. Mercator probably determined the distances between the representations of the parallels in a graphic way (Snyder, 1993).

The mathematical functions for this projection in form of an infinite series were presented by Edward Wright in 1599 and in a finite form in 1668 by James Gregory (Biernacki, 1949).

One of the most significant works for the conformal projections theory was the study by the German mathematician J.H. Lambert, entitled *Anmerkungen und Zusätze zur Entwerfung der Land- und Himmelscharten* which was published in 1772. In Chapter 6, the author provided, for the first time in history, the formulas for the conformal projection of a sphere on a plane. Lambert also presented a differential equation for the conformal projection, which was the basis for deriving the formulas for several projections of this type, including the conical, circular, and transverse cylindrical projection (Biernacki, 1949).

In 1777, the Swiss mathematician Leonhard Euler published in the *Acta Academiae Scientiarum Imperialis Petropolitanae pro anno 1777* three works that discussed cartographic projections, including 2 on conformal projections:

1. *De repraesentatione superficiei sphaericae super plano*,
2. *De projectione geographica superficiei sphaericae*.

First of all, he derived the differential equations based on the general prerequisite of equiangularity, and then presented the functions in various equiangular projections (Biernacki, 1949).

In 1781, Joseph Louis Lagrange (French mathematician and astronomer) published the work entitled: *Sur la construction des cartes geographiques, premier et second memoir*. Lagrange knew the works of Lambert and Euler. He solved the problem of the conformal projection of a rotational surface onto a plane with the use of the method of any function of a complex variable. He also presented the formula for the scale of the projection. Apart from that, he derived the formulas for the circular projection of a rotational surface, followed by deriving the formulas for a sphere and an ellipsoid (Biernacki, 1949).

In 1825, the German mathematician Carl Friedrich Gauss published the work entitled: *Allgemeine Auflosung der Aufgabe: Die Theile einer gegebnen Flache auf einer andern gegebnen Flache so abzubilden, dass die Abbildung dem Abgebildeten in den kleinsten Theilen ahnlich wird*, where he presented the differential equation for the conformal projection of any two surfaces and demonstrated that the problem depends only on the proportionality of the first fundamental forms of the surface theory. Then, he derived the formulas for several simple examples of projections used in geodesy. Moreover, Gauss introduced the term “conformality”, which he used for the first time in 1843, in *Untersuchungen űber Gegenstände der höheren Geodäsie* (Biernacki, 1949).

Another major work in the conformal projections theory was the study by Bernard Riemann, a German mathematician, published in 1851 and entitled: *Grundlagen für eine allgemeine Theorie der Functionen einer complexen veränderlichen Grösse*, where the author addressed the theoretical problem of projecting certain, predefined finite areas on both planes, each of which is enclosed by a defined contour (Biernacki, 1949).

Carl Jacobi, in his study of 1886, entitled *Vorlesungen über Dynamik* (Lectures on Dynamics), proposed a conformal projection of a tri-axial ellipsoid. In order to achieve it, he introduced elliptical coordinates on the tri-axial ellipsoid (Nyrtsov et al., 2014).

### 2.2. Cylindrical projections

As it has already been mentioned, Mercator created his famous world map designed for navigation in 1569. Since that time, this projection has become a standard in creating this type of maps.

A little earlier, in the years 1511–13, Etzlaub created a map of Europe and North Africa in a similar projection (Snyder, 1993).

The conformal transverse cylindrical projection of a sphere onto a plane described by Lambert was generalised for an ellipsoid by Gauss and used for the first time in the years 1820–1830 to calculate the results of triangulation for Hannover. Gauss did not, however, publish the method of the projection. It was presented only later by Oscar Schreiber in his work entitled: *Theorie der Projectionsmethode der hannoverschen Landesvermessung*, published in Hannover in 1866. The method was developed by Louis Krüger in 1912, based on the manuscripts left by Gauss in the publications of the Institute of Geodesy in Potsdam, entitled: *Konforme Abbildung des Erdellipsoids in der Ebene*. On the other hand, the work *Formeln zur Konformen Abbildung des Ellipsoids in der Ebene*, published in 1919 in Berlin by the Prussian Office for Land Surveying, presented formula that were adapted for practical calculations (Różycki, 1973). These formulas allowed calculating the flat rectangular coordinates in narrow meridian belts. The formulas for the whole ellipsoid were derived in 1945 by E.H. Thompson and in 1962 by L. P. Lee with the use of elliptic integrals. The Gauss-Krüger projection (in the USA referred to as the transverse Mercator projection) is currently the basis for creating topographic maps throughout the world. In 1947, Martin Hotine published a work on the oblique cylindrical conformal projections that are a generalisation of the normal and transverse projections. Hotine used the method of double projection, i.e. projecting the ellipsoid onto a sphere and then the sphere onto a plane. He named the projection “orthomorphic”.

The Space oblique Mercator projection was developed in the years 1973–1979 by Colvocoresses, Snyder, and Junkins. This is a conformal projection designed to create maps that consist of satellite images. It is a modified cylindrical projection, where the projection functions are defined by the parameters of satellite orbits (Snyder, 1987).

### 2.3. Azimuthal projections

As it has been already mentioned, normal equiangular azimuthal projections were known as early as in the Ancient era. They were used then to create maps of the sky. This type of projection is believed to have been invented by Hipparchus.

In 1507, the first known map of the world in this projection was created by Walther Ludd (Gaultier Lud) of St. Die, Lorraine. First maps in the oblique projection were also sky maps. In the 4th century AD such map was created by Theon of Alexandria. The first known world map in the oblique azimuthal projection was published in the atlas of Jacques de Vaulx of 1583, while the first world maps in the transverse projection were created in 1542 by Jean Rose. The name “stereographic projection” was first used by the French mathematician François d’Aguilon (1613) in his work *Opticorum libri sex philosophis juxta ac mathematicis utiles* (Sossa & Korol, 2015).

In 1924, the oblique stereographic projection of an oblate ellipsoid was developed by the French astronomer Roussilhe (1924). His work, as numerous later publications, including those by Grabowski (1928), Biernacki (1927), Christov (1964), Letoval'cev (1968), Zenin (1968), and Snyder (1987) provided limited range solutions, usually in the form of the expansion of the mapping functions into power series (Balcerzak, 2000). Balcerzak (2000) developed the functions for mapping the whole ellipsoid and the functions for transformation between the Gauss-Krüger projection and the Roussilhe projection.

### 2.4. Modifications of azimuthal projections, low-distortion conformal projections

Interesting projections are obtained as a result of modifying the stereographic projections: as a result, the lines of constant distortions change their shapes from circles to other curves, which usually reflect the shape of the borders of the mapped area.

Such projection was developed by Miller in 1953 for the area of Europe and Africa, and in 1955 for Central Asia and Australasia. As a result of the polynomial transformation of the stereographic projection, he obtained a map with oval-shaped isolines. Similar projections were used by Reilly in 1973 to create a map of New Zealand and in 1974 by Lee who developed a map of the Pacific Ocean and obtained isolines of more complex shapes, and, finally, by Snyder to create a projection for the map of 48 states of the USA (Snyder, 1987). In 1995, Gonzalez-Lopez created a map of Chile with the use of the polynomial transformation of the transverse Mercator projection (Canters, 2002).

The modified stereographic projections mentioned above may be classified as projections that meet the principle formulated by the Russian scientist Pafnuty Lvovich Chebyshev. In 1853, he formulated the theorem about the "best" cartographic conformal projections that are characterised by the lowest linear distortions. He also provided a criterion that allows minimising the oscillation of linear distortion throughout the projected area. According to Chebyshev's principle, in the class of conformal projections, the projection in which the scale is constant on the edge of the area has the lowest oscillation of the natural logarithm of the length scale. Numerous publications that discuss Chebyshev's theorem and its application for creating projections with a constant scale on the edge of the area include works by: Gdowski (1969, 1971), Nesterov (1997), Balcerzak and Pędzich (1999), Pędzich (1999), Pędzich (2002), and Orihuela (2017). These studies describe methods of creating maps that meet the requirements of Chebyshev's principle for various areas for an oblate ellipsoid. On the other hand, the work (Pędzich, 2019) describes the application of the theorem for mapping areas situated on a tri-axial ellipsoid.

### 2.5. Conic projections

In his work of 1772, Lambert presented the formulas for the conic conformal projection with two standard parallels, both for the ellipsoid and for the sphere. Currently, this projection is commonly used in creating overview topographic maps.

An interesting aspect of the conic projections is the selection of standard parallels. There are several criteria worth mentioning here.

The Ptolemy criterion:

1. The scale has to be minimum at a certain, freely selected parallel,
2. The scale must be equal to one at this parallel.

The De l'Isla criterion:

1. The scales have to be identical on any two selected parallels.
2. The scale must be equal to one at this parallel.

Both these criteria were used in 1772 by Lambert for equiangular conic projections.

The Swiss mathematician Euler proposed the following criteria:

1. The scales have to be equal on two extreme parallels of the area.
2. On the central parallel, the linear distortion has to be equal to the linear distortion on the extreme parallels but with the opposite sign (Biernacki, 1949).

This criterion was used by Witkowski to develop the equiangular conic projection (Fenna, 2007; Różycki, 1973). On the other hand, Kawrajski developed an equiangular conic projection that meets the following criterion: The scales on two extreme parallels of the area have to be identical and equal to the inverse of the scale on the central parallel (Fenna, 2007; Różycki, 1973).

In 1941, Miller and Briesemeister developed a projection named the bipolar oblique conic projection. Two versions of the projection were created. The first one covered South America, with an auxiliary pole in the Pacific Ocean at a point located at the coordinates 20°S and 110°W, and with the standard parallels of the latitudes of 17° and 59°. Then, the projection was used to create another version for North America with the auxiliary pole in the Atlantic Ocean at the coordinates of 45°N and 19°59'36"W and the same standard parallels (Fenna, 2007).

## 2.6. Other interesting conformal projections

Probably the most general conformal projection is the Lagrange projection. It is a generalisation of the projection proposed by Lambert, who projected one hemisphere in a circle, starting from the stereographic azimuthal projection in the transverse position (Fenna, 2007).

Projections that are similar in terms of the graticule were developed by Eisenlohr in 1870 and by August in 1874. They are referred to as two-cusped conformal projections. In creating his projection, Eisenlohr followed the criterion and principle of Chebyshev. August, on the other hand, developed his projection based on an epicycloid, hence the name: August Epicycloidal projection (Fenna, 2007).

In 1833, Littrow developed an equiangular projection where the parallels are projected into ellipses and the meridians into hyperbolas (Szaflarski, 1955).

In 1869, Schwartz proposed a method of transforming a circle into a polygon as well as the transformation of an ellipse into a circle and a sphere into five regular polyhedrons. Later, in 1879, Peirce used these methods as a basis for developing the conformal projection of a sphere onto a plane, where the sphere is projected into a square. This projection is called Quincuncial. Guyon developed a transverse version of this projection in 1886. Later, in 1925, Adams presented several versions of this type of projection: a hemisphere into a regular triangle, regular hexagon, a rhomb, a rectangle, a six-pointed star, and an ellipse (Fenna, 2007).

## 2.7. Conformal projections of a tri-axial ellipsoid

This paper discusses the conformal projections of a tri-axial ellipsoid, which deserve a separate presentation. Some of them, such as the Jacobi projection of a tri-axial ellipsoid, have been mentioned above, but there are more known works on this subject.

Two scientists, in particular, are famous for their studies on conformal projections of tri-axial ellipsoids: Lev Moseevich Bugayevskiy and John Snyder. At this point, it is worth presenting these authors and their works.

Lev Moseevich Bugayevskiy (1921–2010) was a Russian cartographer, a professor at the Moscow Institute of Engineering Geodesy, Aerial Survey and Cartography, Chair of Map Planning and Composition, who dedicated his whole career to mathematical cartography. He was the author of more than 130 publications. In his works he addressed multiple theoretical and practical issues, including, in particular: the general theory of cartographic projections, the distortion theory and projecting one surface onto another, the theoretical basis for the best projections, systems of coordinates, with particular focus on conformal coordinates, transformations of projections, double projections, cartometric calculations, determining the parameters of reference surfaces of extra-terrestrial bodies, the application of projections in creating topographic maps and maps for sea and aerial navigation, the design and terminology of map charts in specific scales, and automation in mathematical cartography, etc. (Lapaine & Divjak, 2017).

Thus, he wrote numerous studies on cartographic projections. In the context of the topic of this paper, the most important aspect of his work is the fact that he was the author of the method of calculating isometric coordinates on a tri-axial ellipsoid. He developed formulas to calculate these coordinates directly on the ellipsoid, without the need to use any additional auxiliary surfaces. He derived general formulas, which, after certain simplifications, may also be used on oblate ellipsoids and spheres. These coordinates may be the basis for developing various types of conformal cartographic projections in compliance with the theory of such projections. The study (Bugayevskiy, 1998) describes the method and provides the formulas for calculating isometric coordinates on a tri-axial ellipsoid. The author also presents a cylindrical projection that was developed based on these coordinates.

On the other hand, John Parr Snyder (1926–1997) was an American scientist. He graduated from the Purdue University and Massachusetts Institute of Technology with an engineer's degree in chemistry. Cartographic projections were his hobby. He was the president of the American Cartographic Association in the years 1990–1991, the secretary of the Washington Map Society, he taught courses on cartographic projections at the George Mason University, but his most famous works were the publications about cartographic projections written for the USGS. He is the author of the Space Oblique Mercator projection, designed for Landsat satellite images, and of the GS50 projection: a minimum distortion conformal projection designed for 50 states of the USA (Lapaine & Divjak, 2017).

Similarly to Bugayevskiy, he was also an outstanding mathematical cartographer. In the context of this paper, the most interesting aspect is the fact that, in 1985, Snyder developed a method of determining the conformal projections of a tri-axial ellipsoid that was slightly different from that proposed by Bugayevskiy and applied so-called conformal coordinates. He also presented an example of applying these coordinates in a cylindrical projection.

Based on Jacobi's projection, Nyrtsov et al. (2014) developed and analysed a transverse cylindrical conformal projection of a tri-axial ellipsoid with the use of elliptic coordinates. A similar projection was also presented by Karney (2017).

The authors of this study intend to determine and present cartographic projections that are based on isometric coordinates and developed according to the method proposed by Bugayevskiy. Snyder's method will be described in our next publications.

## 3. The methodology of developing conformal projections of a tri-axial ellipsoid

### 3.1. Isometric coordinates of a tri-axial ellipsoid according to Bugayevskiy

The study (Bugayevskiy, 1998) describes the method for constructing isometric coordinates on a tri-axial ellipsoid. The data are the semi-axes a,b,c of the tri-axial ellipsoid and the planetographic coordinates B and L. In this paper, only the sequence of formulas used in calculations will be presented.

The following are determined, in sequence:

$$k^2 = 1 - \left(\frac{b}{a}\right)^2, \tag{1}$$

$$d = \frac{b}{\sqrt{1-k^2\cos^2 L}}, \tag{2}$$

$$p^2 = 1 - \left(\frac{c}{d}\right)^2, \tag{3}$$

$$d_L = -\frac{ab\sin 2L\,(a^2-b^2)}{2\,(a^2\sin^2 L + b^2\cos^2 L)^{\frac{3}{2}}}, \tag{4}$$

$$z = -\frac{d_L}{d}. \tag{5}$$

$$\tan B_0 = \tan B\,(1+z^2)^{\frac{1}{2}}, \tag{6}$$

$$\psi_0 = \arcsin(p\sin B_0), \tag{7}$$

$$U' = \frac{\tan\left(\frac{\pi}{4}+\frac{B_0}{2}\right)}{\left(\tan\left(\frac{\pi}{4}+\frac{\psi_0}{2}\right)\right)^p}, \tag{8}$$

$$\tau = \ln U', \tag{9}$$

$$\xi = \tau d, \tag{10}$$

$$\eta = \frac{1}{b}\int_0^{\lambda}\sqrt{d^2 + {d_L}^2}\,d\lambda. \tag{11}$$

The $\eta$ coordinate is calculated with the use of numerical integration methods.

The above formulas are universal and may be used to calculate the isometric coordinates for a tri-axial ellipsoid, an oblate ellipsoid or a sphere. For an oblate ellipsoid, where $a = b$, these formulas are simplified to the form that is commonly applied in cartography for this type of surface. Assuming $a = b = c$, the formulas can be used to calculate isometric coordinates for a sphere.

### 3.2. Initial information and assumptions concerning conformal projections

One of the stages of creating conformal projections consists in introducing isometric coordinates on the reference surface $\xi,\eta$. This enables us to apply the conformal projections theory, according to which any analytical function f of the complex variable that assigns to the isometric coordinates $\xi,\eta$ on the original surface the isometric coordinates $x,y$ on the image area creates a conformal projection:

$$x + iy = f(z) = f(\xi + i\eta) \tag{12}$$

or in the form:

$$x + iy = f(z_r) = f(i\xi + \eta) \tag{13}$$

According to the conformal projections theory (Pędzich, 2019) the scale of length distortions in the projection (12) takes the form:

$$m = \frac{ds'}{ds} = \frac{\left|\frac{df}{dz}\right|}{r(\xi,\eta)} = \frac{\sqrt{x_\xi{}^2 + y_\xi{}^2}}{r(\xi,\eta)} = \frac{\sqrt{x_\eta{}^2 + y_\eta{}^2}}{r(\xi,\eta)} \quad (14)$$

where *ds* is the arc element on the original surface equal to:

$$ds = r(\xi,\eta)\sqrt{d\xi^2 + d\eta^2}$$

and *ds'* is the arc element on the image surface equal to

$$ds' = \sqrt{dx^2 + dy^2}\ .$$

For the tri-axial ellipsoid and the method described here, the formula to calculate *r* has the following form (Bugayevskiy, 1998):

$$r = \sec B_0 \sqrt{1 - p^2 sin^2 B_0}\,\frac{\sqrt{1+z^2}}{\sqrt{1+z^2 cos^2 B_0}} \quad (15)$$

Similar formulas will be obtained for projection (13).

The authors of this article present cylindrical and azimuthal projections, and many others that were developed with the use of the function of the complex variable.

### 3.3. Applied conformal projections

This chapter presents the projection functions in selected conformal projections. Formulas are usually presented in a form that is separated into the real and imaginary parts, i.e. separate formulas to calculate x and y. The authors of this study have decided not to do so, because the functions were implemented in their complex form, and the separation into the real and imaginary parts, if necessary, was performed automatically with the use of the relevant programming functions. This implementation has been described in further sections of the paper.

The authors applied certain known projections, including: normal and transverse cylindrical projections, azimuthal projections, and the Lagrange projection. The application of such functions as sinus and arc sinus, as well as the square root of the complex variable to construct conformal projections was also considered. These functions were selected after a preliminary analysis of a series of complex variable functions.

For the normal cylindrical projection, the projection functions take the following complex form:

$$x + iy = C(\xi + i\eta) = C(z) \quad (16)$$

where *C* denotes a certain value, such as e.g. the radius of the sphere or the length of one of the semi-axes of the ellipsoid, while $\xi,\eta$ are isometric coordinates.

The scale of distortion in such projection takes the following form:

$$m = \frac{C}{r} \quad (17)$$

For the azimuthal projection, the projection functions may be presented in the complex form:

$$x + iy = Ce^{\xi + i\eta} = Ce^{z} \quad (18)$$

The distortion scale equals:

$$m = \frac{C\left|e^{\xi+i\eta}\right|}{r} = \frac{C\left|e^{z}\right|}{r} \quad (19)$$

The Lagrange projection (Orihuela, 2016) takes the form:

$$x + iy = \tan\left(\frac{i\xi + \eta}{2}\right) = \tan\left(\frac{z_r}{2}\right) \quad (20)$$

The distortion scale equals:

$$m = \frac{1}{2r}\left|1 + \tan^2\left(\frac{z_r}{2}\right)\right| \quad (21)$$

The Gauss-Schreiber projection (Orihuela, 2016), i.e. transverse cylindrical projection, takes the form:

$$x + iy = \ln\left(\tan\left(\frac{\pi}{4} + \eta + i\xi\right)\right) = \ln\left(\tan\left(\frac{\pi}{4} + z_r\right)\right) \quad (22)$$

The distortion scale equals:

$$m = \frac{1}{r}\left|\sec(z_r)\right| \quad (23)$$

The application of such complex variable functions as sinus, arc sinus, and the square root was also analysed. The functions were selected after a visual analysis of the obtained cartographic grids that had been drawn for many various analytical functions. The modifications of these functions were also analysed by dividing the argument of the function, i.e. the complex variable, by the constant coefficient *n*.

Projections that apply the sinus function:

$$x + iy = n\sin\left(\frac{\xi + i\eta}{n}\right) = n\sin\left(\frac{z}{n}\right) \quad (24)$$

The distortion scale equals:

$$m = \frac{1}{r}\left|\cos\left(\frac{z}{n}\right)\right| \quad (25)$$

Projections that apply the arcus sinus function:

$$x + iy = n\arcsin\left(\frac{\eta + i\xi}{n}\right) = n\arcsin\left(\frac{z_r}{n}\right) \quad (26)$$

The distortion scale equals:

$$m = \frac{1}{r\left|\sqrt{1 - \left(\frac{z_r}{n}\right)^2}\right|} \quad (27)$$

Projection that applies the square root:

$$x + iy = \sqrt{\eta + i\xi} = \sqrt{z_r} \quad (28)$$

The distortion scale equals:

$$m = \frac{1}{2\left|\sqrt{z_T}\right|} \tag{29}$$

Calculations were performed with the use of the formulas presented above, and then cartographic grids and isolines were developed.

## 4. The algorithm and its implementation in the Octave software

The developed methodology was the basis for developing the algorithm and implementing it in the Octave software. This software is available free of charge and is used for performing calculations and engineering analyses, similarly to the Matlab software. The software is available at www.gnu.org/software/octave/index (GNU Octave, 2022).

The algorithm for calculating the coordinates and the scale of length distortion in conformal projections and for creating the visualisations of cartographic grids and isolines consists of several stages (fig. 1). It will be described on the example of the Lagrange projection.

The first stage consists in data input. These are the lengths of the *a*,*b*,*c* semi-axes and the planetocentric coordinates of points, for which the *x* and *y* coordinates will be calculated in the projection, as well as the length scale *m*. For research purposes, a set of planetocentric coordinates was generated for points that are distributed evenly on the tri-axial ellipsoid at intervals of one degree throughout the whole area of parameters, i.e. φ from –80 to 80 degrees and λ from –150 to 150 degrees. As a result, two tables of planetocentric coordinates were obtained of the dimensions 161 by 301. This task was performed with the use of the *linspace* and *meshgrid* functions (fig. 2).

The next stage consisted in converting the planetocentric coordinates into rectangular coordinates X, Y, Z, and then into planetographic coordinates (fig. 3). This was performed with the use of the equations of the tri-axial ellipsoid as a function of planetocentric coordinates and of planetographic coordinates. Here, the equations described in the work by (Bugayevskiy, 1998) were applied. The transformation of the X, Y, Z coordinates into planetographic coordinates involves a certain problem: at the value of the planetocentric longitude of ±90, an indefinite value of the planetographic latitude is obtained, because the obtained expression

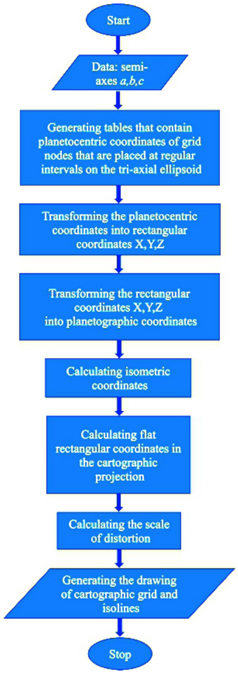


Fig. 1. Diagram of the stages of calculating and visualising cartographic grids and distortions in the conformal projections of a tri-axial ellipsoid

```
clear all;
a=13;  %phobos semiaxis
b=11.39;
c=9.07;

%sets of regular point
no_f=161;
no_l=301;
f=linspace(-80*pi/180,80*pi/180,no_f);
l=linspace(-150*pi/180,150*pi/180,no_l);
[Lam,Fi] = meshgrid(l,f);
```

Fig. 2 Data input and generating the tables with planetocentric coordinates

```
%Transformation from planetocentric coordinates to XYZ coordinates
alfa=1/a;
beta=1/b;
gamma=1/c;
ro=1./sqrt((alfa*cos(Fi).*cos(Lam)).^2+(beta*cos(Fi).*sin(Lam)).^2+(gamma*sin(Fi)).^2);
X=ro.*cos(Fi).*cos(Lam);
Y=ro.*cos(Fi).*sin(Lam);
Z=ro.*sin(Fi);

%Transformation from XYZ coordinates to planetographic coordinates
e2=(a^2-c^2)/a^2;
ea2=(a^2-b^2)/a^2;
L=atan2(Y,(1-ea2)*X);
B=atan2(Z.*cos(L),(X*(1-e2)));
B(:,241)=atan2((1-ea2)*Z(:,241).*sin(L(:,241)),(Y(:,241)*(1-e2)));
B(:,61)=atan2((1-ea2)*Z(:,61).*sin(L(:,61)),(Y(:,61)*(1-e2)));
```

Fig. 3. Converting the planetocentric coordinates into rectangular coordinates X, Y, Z, and then into planetographic coordinates

```
%Calculation of isometric coordinates
k2=1-(b/a)^2;
d=b./sqrt(1-k2*cos(L).^2);
p2=1-(c./d).^2;
dl=-a*b*sin(2*L)*((a^2-b^2)/2)./sqrt((a^2*sin(L).^2+b^2*cos(L).^2).^3);
z=-(dl./d);
B0=atan(tan(B).*sqrt(1+z.^2));
psi0=asin(sqrt(p2).*sin(B0));
Uprim=tan(pi/4+B0/2)./(tan(pi/4+psi0/2).^(sqrt(p2)));
tal=log(Uprim);
ksip=d.*tal;

for jj=1:no_f;
  for ww=1:no_l;
     eta1(jj,ww)=quadcc("eta",0,L(jj,ww))/b;
  end
end

ksi=ksip/b;
```

Fig. 4. Calculating the conformal coordinates

```
function y=eta(L)
  a=13;  %phobos
  b=11.39;
  c=9.07;
  k2=1-(b./a)^2;
  A=(b./sqrt(1-k2.*(cos(L)).^2)).^2;
  Lcz=(a*b*sin(2*L).*((a^2-b^2)./2)).^2;
  M=(a.^2.*(sin(L)).^2+b.^2*(cos(L)).^2).^3;
  B=Lcz./M;
  y=sqrt(A+B);
endfunction
```

Fig. 5. The sub-integral function

is *arctan* $\frac{0}{0}$. This results from the fact that the transformation uses the following relations to calculate the planetographic latitude: $B = arctan\,\frac{Z \cos L}{X(1-e^2)}$, where e is the equatorial eccentricity. For L=±90 the X coordinate equals zero, i.e. the denominator of the fraction equals zero, as well as the numerator. For this value of longitude, a different formula was applied, i.e. = $arctan\,\frac{Z(1-e_a^2)\sin L}{Y(1-e^2)}$, where $e_a$ a is the equatorial eccentricity.

The next stage consists in calculating the isometric coordinates $\xi$ and $\eta$. Calculating the $\eta$ coordinate required the application of the numerical integration method. For this purpose, the Clenshaw-Curtis method was used. The method is available in the Octave software (fig. 4).

The calculations were performed with the use of the eta function. It is a sub-integral function (fig. 5).

Then, the calculated coordinates were denoted in the form of a complex variable (fig. 6) in line 53. The next stage consisted in calculating the flat rectangular coordinates with the use of the complex variable functions, which is calculated with the methods that are already implemented in Octave. The scale of distortions was also calculated (fig. 6).

After that, the cartographic grid was drawn and the isolines were generated (fig. 7). The latter were drawn with the use of the functions: *real* and *imag*, which divide the complex variable function into the real and imaginary parts.

## 5. Data

The source data used here were sets of planetocentric coordinates that had been determined in a regular grid for the tri-axial ellipsoid. These coordinates were later transformed to sets of planetographic coordinates, which were

```
51 %Calculation of x and y coordinates in Lagrange projecion
52
53 Z=eta1+I*(ksi);
54 XY=b*tan(Z/2);
55
56 %linear distortion scale calculation
57 sk=0.5*abs(1+tan(Z/2).^2).*(sqrt(1-p2.*(sin(B0)).^2).*sqrt(1+z.^2)./(cos(B0).*sqrt(1+z.^2.*(cos(B0)).^2)));
58
```

Fig. 6. Calculating the flat rectangular coordinates and the scale of distortions

```
%creation of maps
figure(1);
axis equal;
hold on;

%graticule visualization
delta_f=10;
for ww=1:delta_f:no_f;
  plot(real(XY(ww,:)),imag(XY(ww,:)),'b');
end
delta_l=10;
for ww=1:delta_l:no_l;
  plot(real(XY(:,ww)),imag(XY(:,ww)),'b');
end


%Isolines visualisation
[ccc,hhh]=contour(real(XY),imag(XY),sk,1.00:0.5:7.0,'r');
clabel(ccc,hhh,"fontsize",12);
```

Fig. 7. Drawing the cartographic grid and isolines

used to calculate isometric coordinates and then flat rectangular coordinates.

Due to the fact that the differences between the lengths of the semi-axes were rather significant, the test object used in this study was a tri-axial ellipsoid that is an approximation of the surface of Phobos. Phobos is one of the moons of Mars, which has been studied by cartographers for decades. Parameters of a triaxial ellipsoid as the reference surface of the following semi-major and semi-minor axis length: $a$ = 13.00 km, $b$ = 11.39 km and $c$ = 9.07 km were assumed (Wilner et al., 2010).

## 6. Results and analysis

The isometric coordinates were calculated based on the Bugayevskiy method. However, a major problem was noticed. The $\eta$ coordinate exceeds the range from -$\pi$ to $\pi$. As a result, certain projections require rescaling the $\xi$ and $\eta$ coordinates to adjust the value of $\eta$ to this range.

First, the flat rectangular coordinates were calculated in the cylindrical projection. Based on the calculated coordinates, a cartographic grid was drawn that was limited to the latitude belt of $\varphi \in \langle -60°, 60 \rangle$ with the interval $\Delta\varphi$ = 10° and $\Delta\lambda$ = 10°. In the background, the distribution of length distortions was presented (with the use of the length distortion scale formula) in form of isolines. The results are presented in (fig. 8).

The drawing shows that meridians are represented as straight lines in the equiangular cylindrical projection. The distances between the representations of meridians on the plane are varied, in spite of the same intervals in planetocentric longitude. The central meridian is represented as a section of the x axis of the system of flat rectangular coordinates. The equator is projected as a straight line that is situated on the y axis of the set of flat rectangular coordinates. At the same time, the other parallels are projected in form of curves, whose curvature increases with the growing distance from the projection of the equator. The isolines of length distortions are arranged in a linear form, parallel to the y axis. The equator is projected without any distortions (scale equals 1). The distortions increase with the decreasing distance to the poles (scale is higher than one). Slightly lower distortions may be obtained if the coordinates are multiplied by a constant coefficient, e.g. 0.7, which results in the distortion distribution presented in (fig. 9). In such case, the scale on the equator is 0.7, and reaches one at medium latitudes.

The application of the isometric coordinates according to Bugayevskiy may also help us obtain other projections, such as the azimuthal projection. However, the direct application of the formulas may bring the result presented in (fig. 10).

Such overlapping of the grid results from the fact that the range of the $\eta$ coordinate exceeds the range from -$\pi$ to $\pi$. Thus, the $\eta$ and $\xi$ coordinates should be multiplied by the same constant value in order to obtain a range of the $\eta$ coordinate that falls into the range from -$\pi$ to $\pi$. The projections will remain conformal, but the

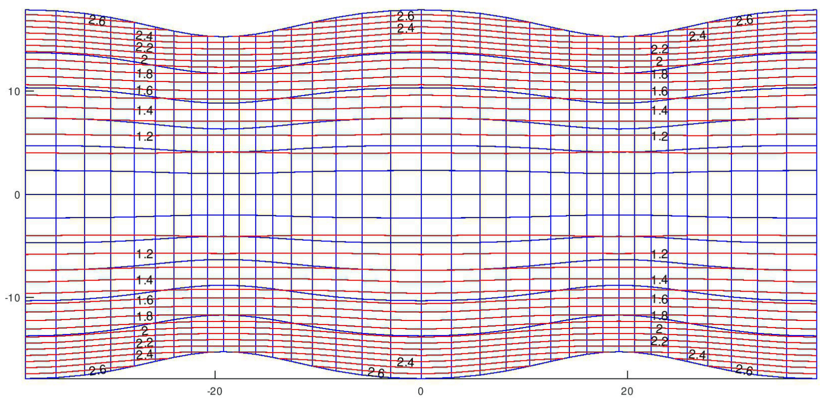


Fig. 8. The cartographic grid and the distribution of distortions obtained in the normal cylindrical projection created with the Bugayevskiy method

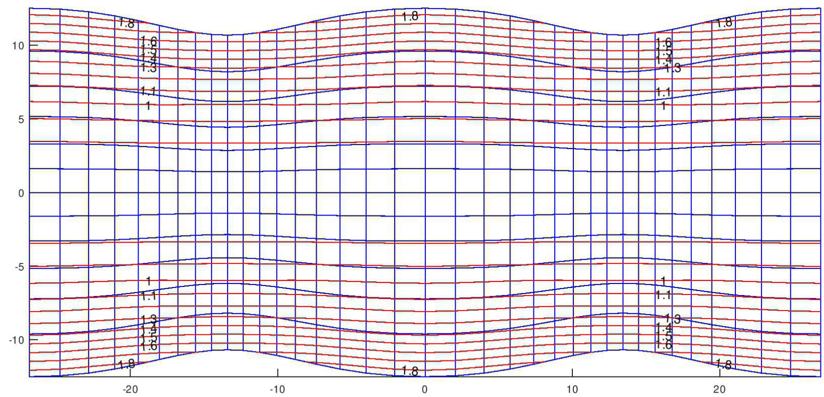

Fig. 9. The cartographic grid and the distribution of distortions obtained in the normal cylindrical projection created with the Bugayevskiy method with a scale coefficient of 0.7

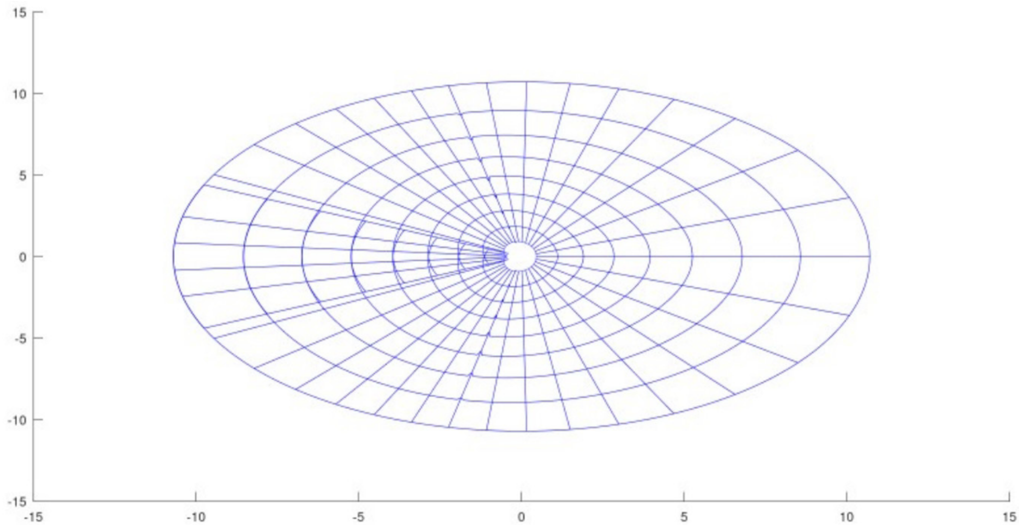

Fig. 10. The cartographic grid in the normal azimuthal projection created based on the isometric coordinates according to Bugayevskiy

cartographic grid will look like the grid presented in (fig. 11). The grid was generated for the southern hemisphere, because, according to formula 18, the south pole is projected in the origin of the system of coordinates. In order to project the north pole in the origin of the system of coordinates, the η coordinate should be preceded by a minus sign. The projections of the parallels take an elliptic shape, which becomes more similar to a circle with the decreasing distance from the pole. The distribution of distortions is interesting: on the equator, the scale of distortion equals one and decreases towards the pole. This may be modified by multiplying the projection functions by a constant value, e.g. 2.

Another projection analysed in this article is the Lagrange projection. Figure 12 presents the cartographic grid and the distribution of distortions in this projection. This time, the grid was limited to the planetocentric latitudes from -80 to 80 degrees and the longitudes from -150 to

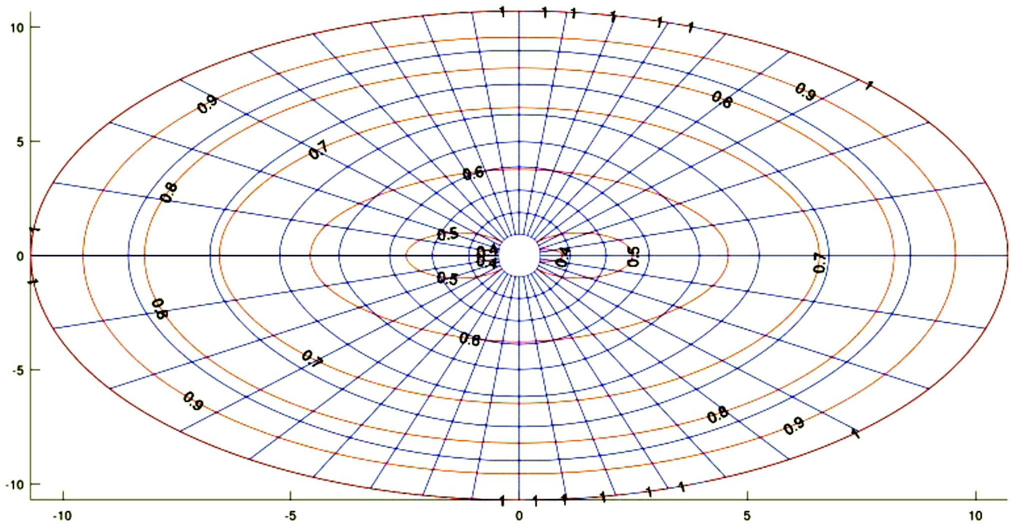


Fig. 11. The grid and distribution of distortions obtained in the azimuthal projection. The grid is limited to latitudes from 0 to 80 and longitudes from -180 to 180. It is drawn with 10 degree intervals

150 degrees. The projections of meridians and parallels have circular or elliptic shapes. The shapes of isolines also resemble circles, with the centre at the centre of the map.

Figure 13 presents the cartographic grid and the distribution of distortions in the Gauss-Schreiber projection. The grid was drawn for the planetocentric latitudes from 0 to 80 degrees and the longitudes from -180 to 180. The southern hemisphere is projected in a similar way. This projection may be considered to be a transverse cylindrical projection. The distribution of distortions is interesting. As the distance from the projection of the pole increases, the

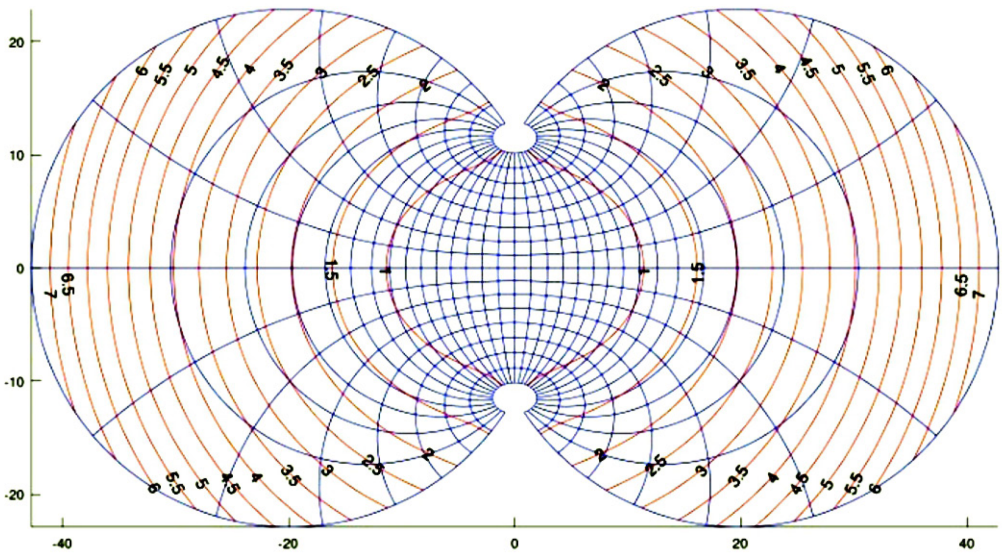


Fig. 12. The cartographic grid and the distribution of distortions in the Lagrange projection

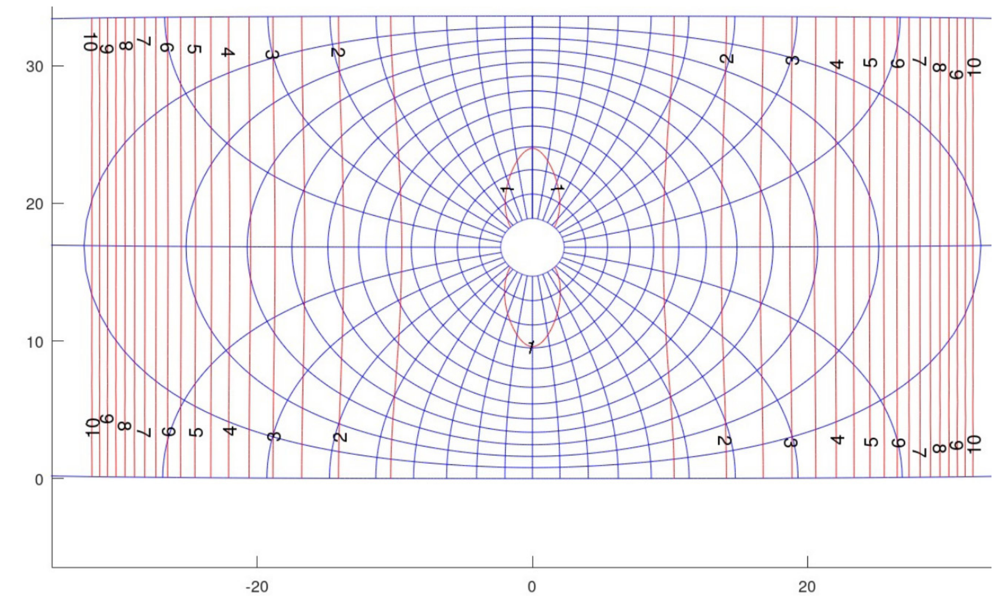


Fig. 13. The cartographic grid and the distribution of distortions in the Gauss-Schreiber projection

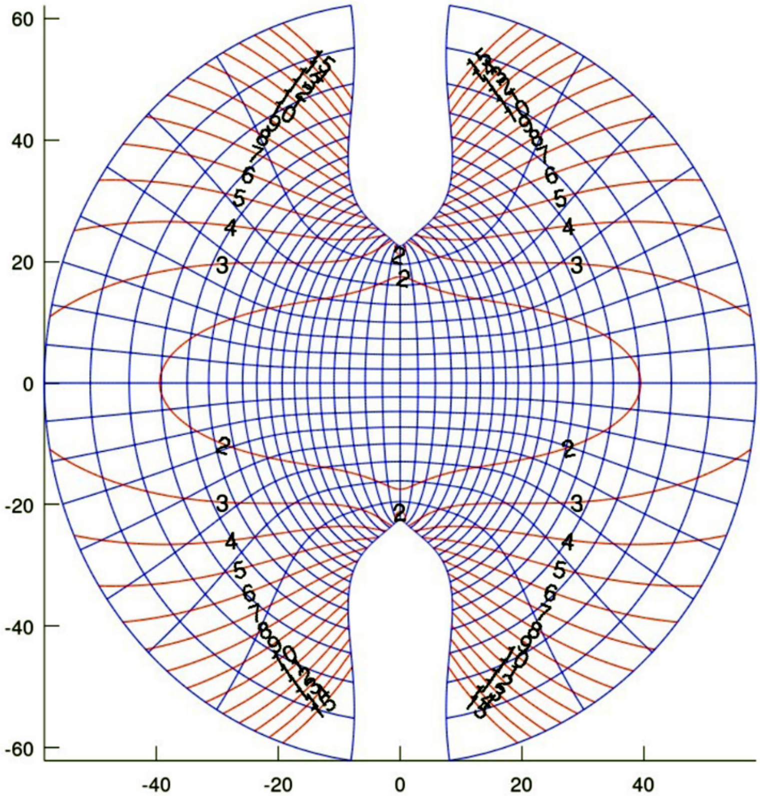


Fig. 14. The cartographic grid and the distribution of distortions in the projection with the use of the function 2 sin $\frac{z}{2}$

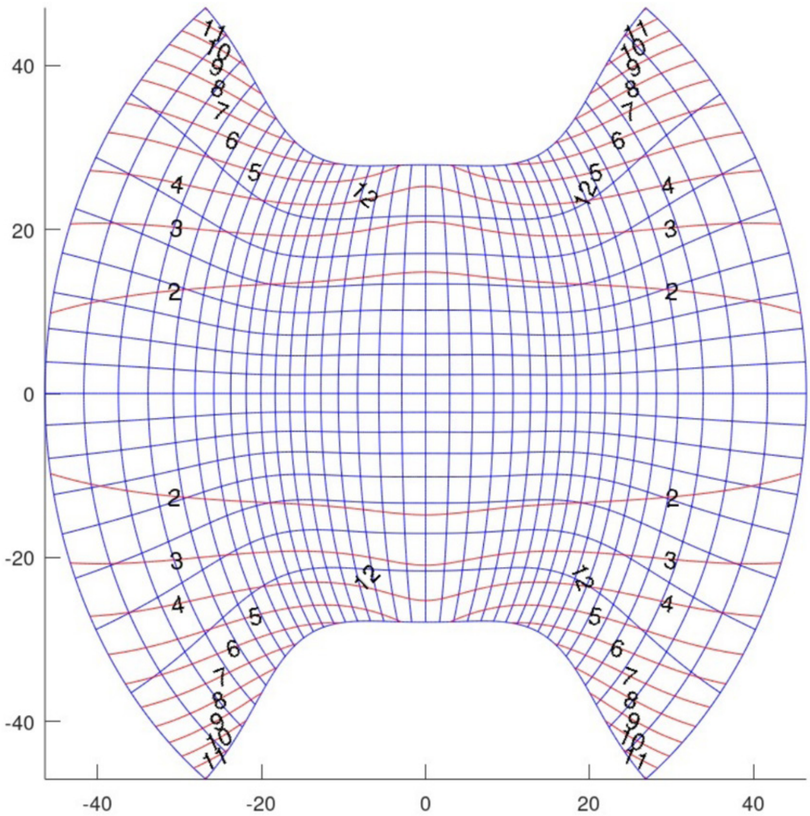

Fig. 15. The cartographic grid and the distribution of distortions in the projection created with the use of the function $3 \sin \frac{z}{3}$

shapes of isolines become increasingly similar to straight lines. Their curvature increases in the proximity of the projection of the pole.

For the sinus function, formulas (24) and (25) were applied to generate several grids and isolines of distortion in the range of coordinates from -80 to 80 degrees of planetocentric latitude and from -180 to 180 for planetocentric longitude, adopting different values of the n coefficient.

For $n$ = 2, the grid and distribution of distortions presented in (fig. 14) were obtained. The result is very interesting. The areas located near the poles are extremely distorted, so that the potential application should be limited to certain ranges of geographic latitudes and longitudes.

As the value of the n coefficient increases, the obtained grids become more and more similar to those in cylindrical projections. This is obvious, as the obtained values of the arguments of the function, for which the values of the function become more similar to those in cylindrical projection, are decreasing. The grid for $n$ = 3 is presented in (fig. 15), and for $n$ = 8 in (fig. 16).

For the arcus sinus function, formulas (26) and (27) were applied to generate several grids and isolines in the range of coordinates from -80 to 80 degrees of planetocentric latitude and from -180 to 180 for planetocentric longitude, adopting different values of the $n$ coefficient. Selected grids and distribution of distortions are presented in the illustrations below. The grid for $n$ = 3 is presented in (fig. 17), for $n$ = 4 in (fig. 18), and for $n$ = 8 in (fig. 19). Here, one may also conclude that, as the value of the $n$

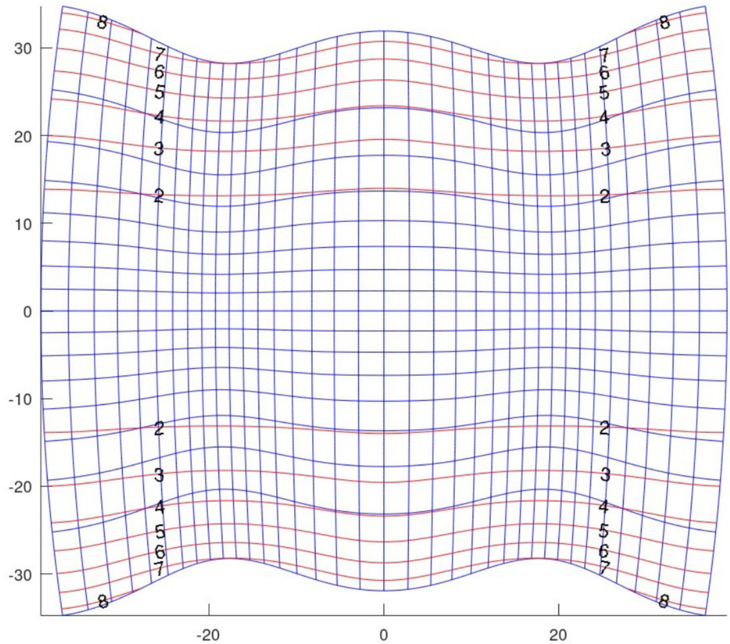


Fig. 16. The cartographic grid and the distribution of distortions in the projection created with the use of the function $8 \sin \frac{z}{8}$

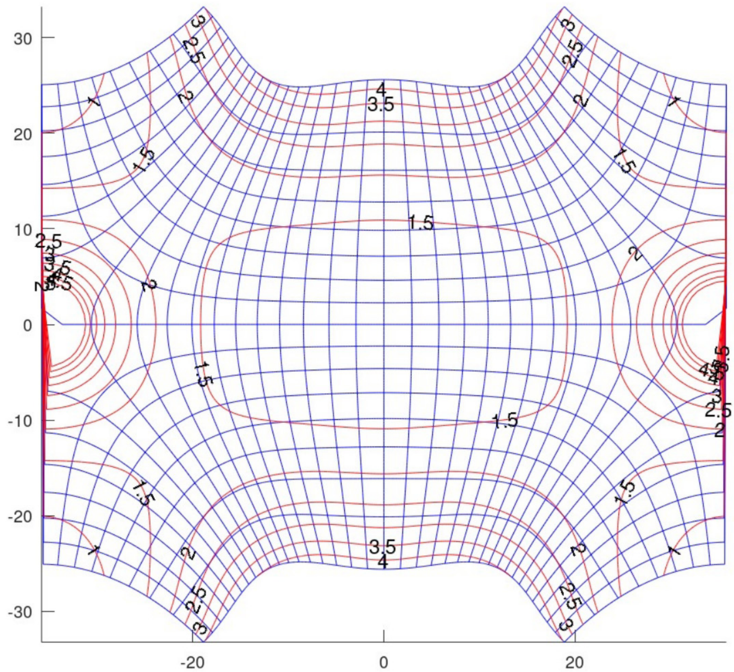


Fig. 17. The cartographic grid and the distribution of distortions in the projection created with the use of the function $2 \arcsin \frac{z}{2}$

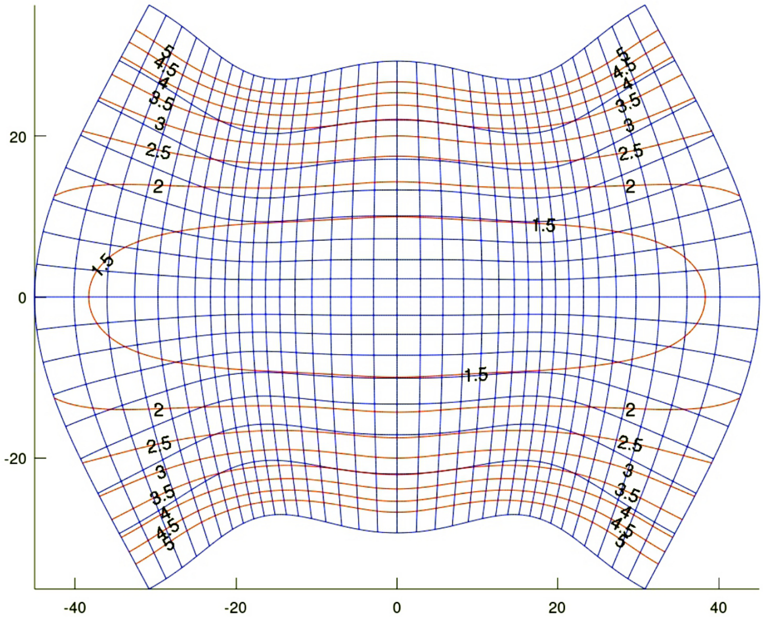


Fig. 18. The cartographic grid and the distribution of distortions in the projection created with the use of the function $4 \arcsin \frac{z}{4}$

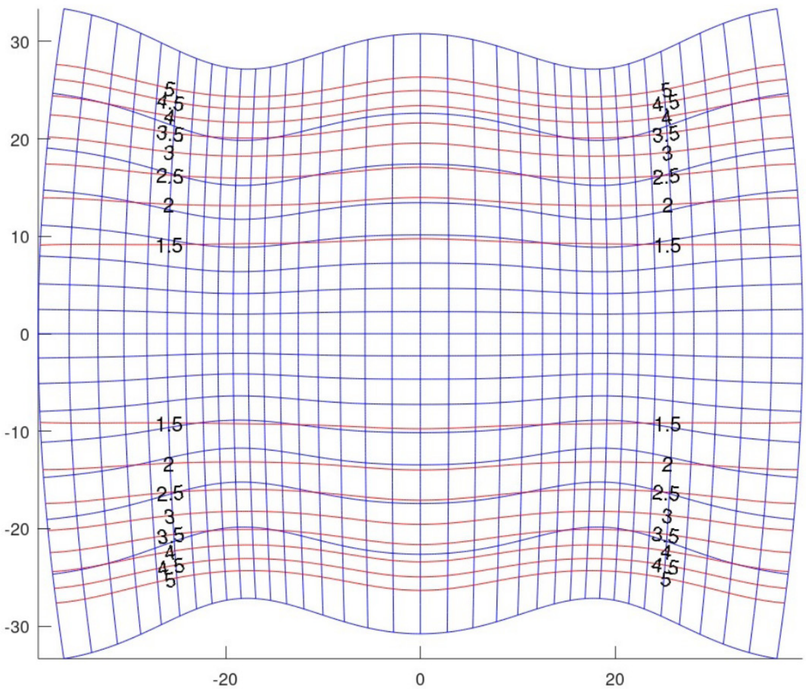


Fig. 19. The cartographic grid and the distribution of distortions in the projection created with the use of the function $8 \arcsin \frac{z}{8}$

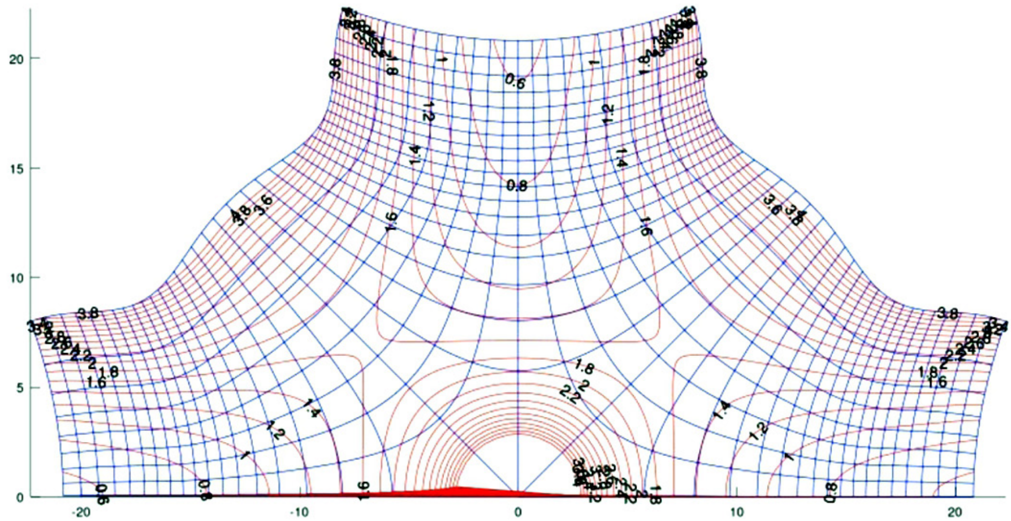

Fig. 20. The cartographic grid and the distribution of distortions in the projection created with the use of the square root function

coefficient increases, the obtained grids become more and more similar to those in cylindrical projections. For the coefficient value $n$ = 8 the grids in (fig. 16) and (fig. 19) are very similar.

Grids were also developed for projections that were created with the use of other functions. However, the obtained results either resembled the previous ones, or were rather unusual, as those presented in (fig. 20). It presents the cartographic grid and the distribution of distortions in the projection created with the use of the square root function. The cartographic grid was drawn for the planetocentric latitudes ranging from -80 to 80 and longitudes from -180 to 180. The obtained result was rather unusual. In this projection, the equator is projected in form of three fragments, one of which is parallel to the x axis, while the other two are parallel to the y axis.

## 7. Conclusion

The paper presents the methodology for creating conformal projections of a tri-axial ellipsoid with the use of isometric coordinates. Apart from that, the possibilities to implement this methodology in the Octave software are presented. The authors described the properties of selected conformal projections. For this purpose, cartographic grids and isolines of distortion were developed.

The paper demonstrates that performing the calculations and creating visualisations of data in conformal projections of a tri-axial ellipsoid are not difficult tasks. Unfortunately, popular GIS packages do not offer the possibility to create these types of projections. The implementation of these projections in GIS software would enhance them by providing additional functionalities.

## Literature

Balcerzak, J. (2000). Uogólnione odwzorowanie Roussilhe'a powierzchni elipsoidy. *Prace Naukowe Politechniki Warszawskiej. Geodezja*, (37), 3–65.

Balcerzak, J., & Pędzich, P. (1999). Quest for a cartographic projection of the Chebyshev type in the domain of analytic functions of complex variable. Theoretical foundations. *Geodezja i Kartografia, 48*(3–4), 75–85.

Biernacki, F. (1927). Odwzorowanie Roussilhe'a i próba zastosowania jego metody do obszaru Polski. *Biblioteka Przeglądu Mierniczego*, (12).

Biernacki, F. (1949). *Teoria odwzorowań powierzchni*. Główny Urząd Pomiarów Kraju.

Bugayevskiy, L. M. (1987). K voprosu o poluchenii izometricheskikh koordinat i ravnougol'noy tsilindricheskoy proyektsii trekhosnogo ellipsoida. *Izvestiya*

*Vysshikh Uchebnykh Zavedeniy. Geodeziya i Aerofotosyemka*, *4*, 79–90.

Bugayevskiy, L. M. (1991). Izometricheskiye koordinaty, ravnougol'noy tsilindricheskoy, konicheskoy i azimutal'noy proyektsii trekhosnogo ellipsoida. *Izvestiya Vysshikh Uchebnykh Zavedeniy. Geodeziya i Aerofotosyemka*, *3*, 144–152.

Bugayevskiy, L. M. (1998). *Matematicheskaya kartografia*. Zlatoust.

Canters, F. (2002). *Small-scale Map Projection Design*. Taylor & Francis.

Christov, V. (1964). *Matematyczeska Geodezja*. Technika.

Fenna, D. (2007). *Cartographic science. A compendium of map projections with derivations*. CRC Press, Taylor & Francis Group.

Gdowski, B. (1969). *Minimalizacja zniekształceń w odwzorowaniach powierzchni*. Oficyna Wydawnicza Politechniki Warszawskiej.

Gdowski, B. (1971). O pewnej metodzie konstrukcji odwzorowań Czebyszewa. *Geodezja i Kartografia*, *20*(2).

GNU Octave. (2022). www.gnu.org/software/octave/index

Grabowski, L. (1928). O odwzorowaniach płaskich wiernokątnych elipsoidy obrotowej, w których pewien wybrany południk odwzorowuje się jako linia prosta. *Czasopismo Techniczne*.

Hotine, M. (1947). The orthomorphic projection of the spheroid–III. *Empire Survey Review*, *9*, 52–70. https://doi.org/10.1179/sre.1947.9.64.52

Karney, C. F. F. (2017). *GeographicLib, Version 1.49*. https://geographiclib.sourceforge.io/1.49

Lapaine, M., & Divjak, A. K. (2017). Famous People and Map Projections. In M. Lapaine & E. Lynn Usery (Eds.), *Choosing a map projection* (pp. 259–326). Springer.

Letoval'cev, I. G. (1968). O projekcji Rusilja. *Izwiestia, Godezja i Aerofotosiemka*, *2*.

Nesterov, I. G. (1997). CAMPREL: a new adaptive conformal cartographic projection. *Cartography and Geographic Information Systems*, *24*(4), 221–227. https://doi.org/10.1559/152304097782439295

Nyrtsov, M., Fleis, M., Borisov, M., & Stooke, P. (2014). Jacobi Conformal Projection of the Triaxial Ellipsoid: New Projection for Mapping of Small Celestial Bodies. In M. Buchroithner, N. Prechtel & D. Burghardt (Eds.), *Cartography from Pole to Pole* (pp. 235–246). Springer Berlin Heidelberg.

Orihuela, S. (2016). Generalization of the Lambert–Lagrange projection. *The Cartographic Journal*, *53*(2), 158–165. https://doi.org/10.1080/00087041.2015.1108063

Orihuela, S. (2017). Optimal conformal map projections in harmonic polynomials in terms of Gauss-Schreiber coordinates. *Survey Review*, *49*(354), 227–236. https://doi.org/10.1179/1752270615Y.0000000042

Pędzich, P. (1999). Power series approximation of a projection of the Chebyshev type of the area of Poland. *Geodezja i Kartografia*, *48*(3–4), 87–96.

Pędzich, P. (2002). *Opracowanie odwzorowania kartograficznego o optymalnym rozkładzie zniekształceń według kryterium Czebyszewa dla ograniczonego obszaru powierzchni elipsoidy* [PhD thesis]. Warsaw University of Technology.

Pędzich, P. (2017). Equidistant map projections of a triaxial ellipsoid with the use of reduced coordinates. *Geodesy and Cartography*, *66*(2), 271–290. https://doi.org/10.1515/geocart-2017-0021

Pędzich, P. (2019). A low distortion conformal projection of a tri-axial ellipsoid and its application for mapping of extra-terrestrial objects. *Planetary and Space Science*, *178*. https://doi.org/10.1016/j.pss.2019.104697

Pędzich, P., & Latuszek, K. (2014). Kartografia planetarna – przykłady opracowań, odwzorowania kartograficzne, nowe wyzwania. *Polski Przegląd Kartograficzny*, *46*(4), 369–396.

Roussilhe, H. (1924). *Cours d'astronomie appliquèe et gèodèsie*. Librairie de l'Enseignement Technique.

Różycki, J. (1973). *Kartografia matematyczna*. Państwowe Wydawnictwo Naukowe.

Snyder, J. P. (1985). Conformal mapping of the triaxial ellipsoid. *Survey Review*, *28*(217), 130–148.

Snyder, J. P. (1987). *Map projections. A working manual*. United Government Printing Office.

Snyder, J. P. (1993). *Flattening the Earth. Two Thousand Years of Map Projections*. University of Chicago Press.

Sossa, R., & Korol, P. (2015). Historical Aspects of Development of the Theory of Azimuthal Map Projections. *Studia Geohistorica*, *3*, 187–203. https://doi.org/10.12775/SG.2015.13

Szaflarski, J. (1955). *Zarys kartografii*. PPWK.

Wilner, K., Oberst, J., Hussmann, H., Giese, B., Hoffmann, H., Matz, K.-D., Roatsch, T., & Duxbury, T. (2010). Phobos control point network, rotation, and shape. *Earth and Planetary Science Letters*, *294*(3–4), 541–546. https://doi.org/10.1016/j.epsl.2009.07.033

Zenin, V. N. (1968). K voprosu o vybore geodezicheskoy projekcji dla izhenerno-geodezicheskich robot. *Izvestiya Vysshikh Uchebnykh Zavedeniy. Geodeziya i Aerofotosyemka*, *6*.